The International Journal of Advanced Manufacturing Technology (2018) 99:1379–1387
https://doi.org/10.1007/s00170-018-2595-4

ORIGINAL ARTICLE

Experimental, numerical, and analytical investigations on the charge weld evolution in extruded profiles

Barbara Reggiani[1] · Lorenzo Donati[2]

Received: 29 March 2018 / Accepted: 15 August 2018 / Published online: 22 August 2018

Abstract

Charge welds are unavoidable product defects generated during the continuous extrusion of metallic materials that extend to a certain variable length and that are marked by lower mechanical properties than the base material. The portion of the profile containing the charge welds thus needs to be scrapped and an accurate prediction of this portion becomes mandatory, not only for the final user of the profile, in order to avoid in-service product failures, but also for extruders and die makers in order to increase the process efficiency. In the present work, four case studies carried out in the years by the authors on the prediction of the charge weld extension are reviewed and systematically compared in terms of experimental and numerical results. Data are furthermore compared with the predictions of analytical models reported in literature for the scrap length calculation and of an industrial empirical rule based on the extrusion ratio. Final aim of the work is to highlight potentials and limits of each predictive method and to assess their applicability in the everyday industrial practice.

Keywords Charge weld · Extrusion · Scrap minimization · Analytical model · Finite element model

1 Introduction

The direct extrusion of aluminum alloys is a widely used manufacturing process due to its high productivity and flexibility. However, the extruded profiles are marked by different types of defects, some of which are of primary importance for structural applications since they influence the final mechanical properties of the product. Specifically, seam and charge welds, together with the billet skin (or back-end) defect, represent potential scathe for the extruded profile if not properly predicted and ruled [1].

Seam welds, also known as longitudinal seams, are characteristic of hollow and semi-hollow profiles that require a second tool more than the die, i.e., the mandrel. The die gives the external shape to the profile and the mandrel to the internal one. In order to provide a physical support to the mandrel, a certain number of legs are used. This implies that the flowing material of the billet is initially divided around the mandrel legs; then, it rejoins in the welding chamber producing the seam welds, one for each leg [2, 3]. A primary consequence of this generating process is that seam welds cannot be avoided in case of hollow or semi-hollow profiles and extend all along the entire profile length. However, seam welds can exhibit the same strength of the base material if the die design and the process parameters are properly selected [4].

The back-end defect consists in the presence of the billet skin inside the final profile and it affects both solid and hollow profiles [5]. Due to the high friction at the billet-container interfaces, the skin adheres to the container during the extrusion process and it is progressively scraped by the ram and accumulated at the back-end of the billet. The skin of the billet is usually marked by a different chemical composition or microstructure with lower mechanical properties than the inner material. This difference either can be the result of an altered chemical composition (because of cooling from casting) or of a contamination due to impurities (oxides, dust, oil, etc.) collected during billet shipping, pre-heating, and loading into the press. Some studies are reported in literature concerning the flow behavior of the billet surface layer [5–11]. However, a certain work still has to be done in order to properly predict the

✉ Barbara Reggiani
barbara.reggiani@unimore.it

[1] DISMI Department of Sciences and Methods for Engineering, University of Modena and Reggio Emilia, Via Amendola 2, 42122 Reggio Emilia, Italy

[2] DIN Department of Industrial Engineering, University of Bologna, Viale Risorgimento 2, 40136 Bologna, Italy

billet skin impact on the process, both in terms of thickness definition of the skin and of the experimental and numerical assessment of this type of defect. What is instead shared knowledge is that the key parameter used to control billet skin contamination is the length of the discarded butt. Specifically, the billet skin defect can be controlled by selecting an optimal butt length where a longer rest allows holding more billet skin and consequently it guarantees a profile free from contaminants, while a shorter rest reduces the material losses.

Coming to the focus of the present work, charge welds, also called transverse welds or front-end defects, are always portions of the profile with lower mechanical properties than the base material [12]. Indeed, at the end of each process stroke, the back end of the old billet material that completely fills the die starts to interact with the front side of the new billet loaded into the press that is usually contaminated by oxides, dust, or lubricant thus producing a transition zone that extends to a certain variable length [13, 14]. Charge welds extend in the extrusion direction before the stop-mark, which is an evident mark on the profile surface generated by the material adhesion on the bearing zones during the billet change. In Fig. 1, the longitudinal section of an extruded round bar containing a charge weld is schematized, the darker zone representing the incoming new billet, and the lighter one as the old billet material [14]. The charge weld onset is the beginning of the transition zone in which almost 100% of the profile section is still made of the old billet material. The onset appears at a certain distance from the stop mark and the charge weld exhausts to a variable length when the new billet has nearly integrally replaced the old one. The charge weld evolution (d) is the distance of the exhausting point from the stop mark.

Different from the back-end defect but similar to the seam welds, charge welds are unavoidable parts of extruded products. Nevertheless, as previously stated, contrarily from the seam welds, the mechanical properties of the charge welds are always lower than those of the base material.

The evolution of the mechanical properties of the charge welds as a function of the old-new billet replacement has been investigated in literature [12, 13, 15] as well as the detrimental effect of the charge welds on the fatigue life of the final product [16]. The aim of these works was to reduce the unnecessary scrap by detecting the impact of each portion of the transition zone on the in-service performances of the profile. Only a single study reports a simplified analytical formulation for the estimation of the minimum expected charge weld strength computed as a percent of the ultimate tensile strength of the base material and as a function of the extrusion ratio [17]. However, the applicability of this formula is limited to simple solid profiles in ideal conditions such as clean billets, clean butt shearing, and metal not stripped by butt shearing, conditions that are far from those of an industrial extrusion implant. In addition, the previous studies clearly emerged that the decay of the mechanical properties starts immediately close to the charge weld onset and comes back to the base material properties only near the exhausting point.

It comes then clear that the entire length of the profile containing charge welds needs to be scrapped and that an accurate prediction and reduction of this portion are mandatory. This would be beneficial not only for the final user of the profile in order to avoid in-service product failures, but also for extruders and die makers to increase process efficiency by reducing unnecessary scraps. It is reported in literature that the way of interaction and replacement of the old-new billet is primarily influenced and driven by the die geometry [13, 18–21]. Other process parameters such as profile alloy, billet pre-heating temperature, extrusion speed, and friction level have been reported to be negligible factors in the definition of the charge weld onset and extension [21–25]. However, further and deeper investigations are required on this matter.

The methodologies that can be used for the charge weld length assessment are, basically, experimental, numerical (by means of finite element analyses), and analytical. However, the experimental determination of the charge welds is known to be a time consuming activity that requires the slicing and etching of the profile; in addition, the achieved conclusions are circumscribed to the specific investigated geometry. Thus, a breakthrough in the understanding and prediction of the charge weld phenomenon came from the use of numerical approaches. Contrary from experiments, numerical models allow investigating many different die designs for a specific profile in a reduced time with respect to an experimental campaign.

In the last decade, a lot of work has been done on the use of numerical models applied to the extrusion process of aluminum profiles, which has been simulated by means of finite element (FE) codes [26, 27]. However, the studies specifically dedicated to the charge welds that make use of numerical modeling tools are limited. Qiang et al. [28] and Mahmoodkhani et al. [24] performed FE simulations of the charge weld phenomenon by means of Lagrangian codes. Both investigations, however, used only 2D FE models and very simplified profile shapes due to the high computational cost of the Lagrangian approach, making the extension of the results to more complex geometries a difficult task. In addition, no experimental validation was performed in terms of charge weld formation and evolution. Later, Mahmoodkhani et al. [24] computed the thickness and length of the charge weld transition zone for different feeder dimensions and validated the calculation against industrial data on a simple solid bar. From 2013, the capability of a commercial FE code to predict the charge weld extension for a complex 3D multi-hole porthole die has been verified, finding a good agreement between experimental and numerical data in terms of evolution of the phenomenon and scrap length [20, 23, 25, 29]. In addition to numerical models, also analytical formulations have been proposed in the past for a fast computation of the charge welds. To the author's knowledge, two formulas are nowadays

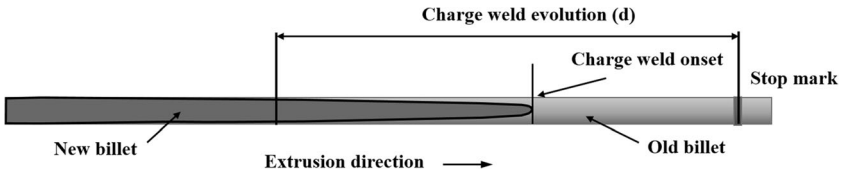

Fig. 1 Extrusion length with a transition zone (charge weld)

present in literature. The first one has been presented in 2008 [30]:

$$d = \frac{(V_1 + V_2)}{A_E \cdot n} \tag{1}$$

in which d is the charge weld evolution (Fig. 1), V_1 and V_2 are the total volume of the metal left in the die ports and in the weld chambers, respectively, from the old billet, A_E is the cross-sectional area of the extruded profile, and n is the number of holes in the die.

The second formula is an adjustment achieved by multiply the ratio in Eq. 1 of a 1.5 factor [11]:

$$d = 1.5 \cdot \frac{(V_1 + V_2)}{A_E \cdot n} \tag{2}$$

As reported in [11], the corrective factor of 1.5 is the result of two main considerations. Firstly, the volume of metal that leaves the die at the start of the next billet is less than the port volume, varying from 60 to 90% of the port volume because of the dead metal zones. Second, the metal in the die does not leave as a simple plug but moves a lot faster in the center of the ports with a gradual clearing at the outside. The last portion of the material that is replaced is that near to the seam welds and at on the external surface of the profile suggesting a doubling of the prediction made with Eq. 1. The combined effect of these two contributions equates to about 150%, thus giving the 1.5 coefficient in Eq. 2.

Currently, due to this limited literature and in consideration of the fact that FE codes are still not a standard in industry, determination of the zone to be discarded in everyday practice for charge weld contamination is still performed by means of intuition, analogy with similar profile shapes, and experience. It is a frequent industrial practice to discard 1000 mm of profile before the stop mark for skin contamination and a profile length after the stop mark in relation to the extrusion ratio R for the presence of the charge welds. As a guideline, 1000 mm for $R < 30$, 2000 mm for $30 < R < 40$, and 3000 mm for $R > 40$ are scrapped with R being the extrusion ratio.

In this scenario, the aim of the present work was to compare the experimental-numerical investigations performed in the years by the authors in terms of charge weld extensions with the outcome of Eqs. 1 and 2 and with that of the empirical rule based on the extrusion ratio R. In detail, four case studies have been taken into account for which only partial comparisons were previously already reported in literature. For the first and the second case study, the comparison with the adjusted Eq. 2 and with both Eqs. 1 and 2 respectively was still not reported, while for the third case study, what was missing was the predictions achieved with Eqs. 1 and with the empirical rule. For the last (fourth) case study, only the experimental investigation was previously published. To the best of the authors' knowledge, no previous published study reports such a comprehensive assessment of the charge welds in extruded products. Four case studies should be considered a robust database in consideration of the complex industrial setting required to collect all the information and of the long time need to perform both the experimental and numerical assessment of the charge welds. Final aim of the work was to highlight potentials and limits of each predictive method and to assess their applicability in the everyday industrial practice.

2 Case study 1: multi-profile extrusion

In the first study, a multi-hole die used to produce four hollow profiles (in the following referred as A, B, C, and D) was investigated (Fig. 2a) [23]. The geometry of each profile was composed by a massive part and a thin long tongue (Fig. 2b). The inner cavity was produced by a mandrel supported by two bridges. A non-symmetrical position of the profiles, with respect to the horizontal axis of the die, allowed investigating the influence of holes placement and orientation on metal flow (profiles A–D have the massive part of the section towards the center of the billet, unlike profiles C–B) while the vertical symmetry allowed FE computation of half the process due to symmetry. The extrusion ratio (E.R.) was equal to 50. Four billets made of an AA6060 alloy were extruded consecutively during the experimental investigation in order to achieve a steady-state condition. The FE model was generated and evaluated by means of a transient (time-dependent) analysis performed on the ALE code Altair HyperXtrude [31] and the total simulation time was 132 h. The same FE code and the same type of transient analysis were used to perform all the numerical investigations reported in the present work.

The experimental-numerical comparison for the profile A in terms of percentage of old-new material replacement as a function of the distance from the stop mark is reported in Fig. 3. It can be seen the very good numerical-experimental agreement achieved both in terms of onset and exhausting point of the charge weld and in terms of general trend.

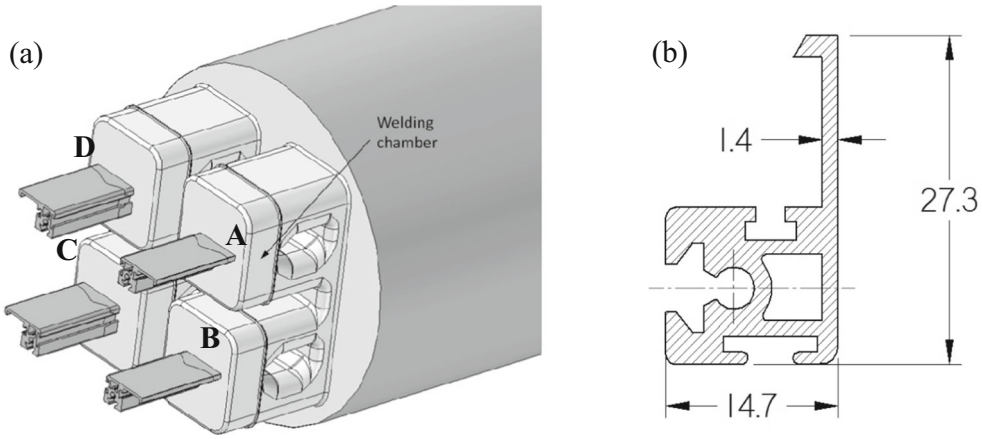

Fig. 2 **a** The die used for the first case study with the profile labeling and **b** profile shape [23]

Experimentally, it was found that the four charge welds of the profiles evolved differently. Specifically, it was found that the charge welds started at different distances from the stop mark for the different profiles in the range of 400 to 550 mm. Furthermore, the complete transition length (d in Fig. 1) of the phenomenon strongly varied from 1550 mm for profile C to the 2100 mm of profile D (Table 1).

The die design, in particular the feeding ports dimension or the localization of the profiles on the die, together with their orientation, had a great effect on the velocity unbalance. Profiles A and D showed the greatest transition length because their thinner sections were located at a greater distance from the die center (which causes a slower material flow). Noting the die symmetry, same results should have been found for symmetric profile, that is between A and D on the top and between B and C on the bottom. Differences between the two sides were indeed small and had a maximum value of 100 mm between the start of the weld in B and C profiles. The performed simulation was able to properly predict a different evolution of profiles A and B.

The obtained charge weld evolution was compared to the analytical results of Eqs. 1 and 2 (Table 1). No specific analytical computations were made for each profile even if fed by different die ports. This is because in the industrial practice, it is difficult to properly anticipate the exact portion of the profile cross-section fed by each port since it can significantly vary from what was expected due to the complex material flowing inside the die. Thus, in consideration of the final goal of the present work that aimed at assessing the applicability of the predictive methods in the industrial practice, a single value of the transition length was evaluated.

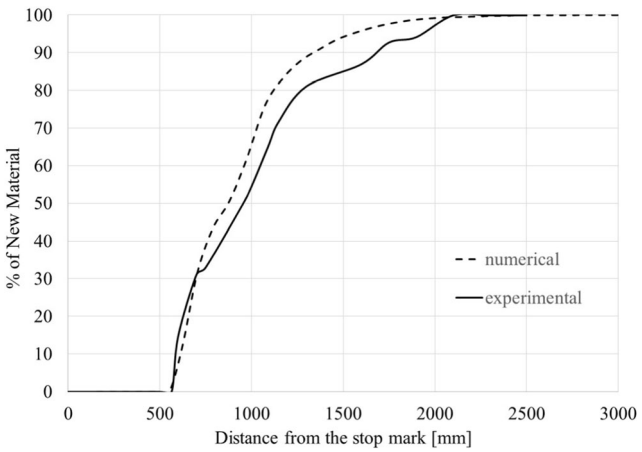

Fig. 3 Numerical-experimental comparison of the charge weld evolution for profile A [23]

The empirical rule based on the extrusion ratio, with an E.R. of 50, suggested a length of profile to be scrapped equal to 3.000 mm.

From Table 1, it emerges that Eq. 1 returned a charge weld length of 1252 mm, less than the minimum experimental value of 1550 mm for profile C and significantly less than that of profile D; the one with the longest transition. On the contrary, the empirical rule based on the extrusion ratio suggested a length of 3000 mm, much more than the peak value of 2100 mm, thus leading to an overestimation of the material to be scrapped of 42%. Eq. 2 predicted a scrap length of 1859 mm. If this value compared with the single experimental evolutions led to quite high percentage errors (11% for profile D, 19% for profile C, A and B in the middle), globally, it well matched with the experimental average of 1800 mm. Even stating this consideration, if translated at an industrial level, an erroneous estimation of the charge weld extension of ±

Table 1 Numerical-experimental-analytical charge weld extensions (d in Fig. 1) for the first case study (in mm)

Experimental	Numerical (FE)	Analytical		E.R. rule
		(Eq. 1)	(Eq. 2)	
1950 (profile A) 1600 (profile B)	1790 (profile A) 1397 (profile B)	1252	1858	3000
1550 (profile C)				
2100 (profile D)				
Avg: 1800				

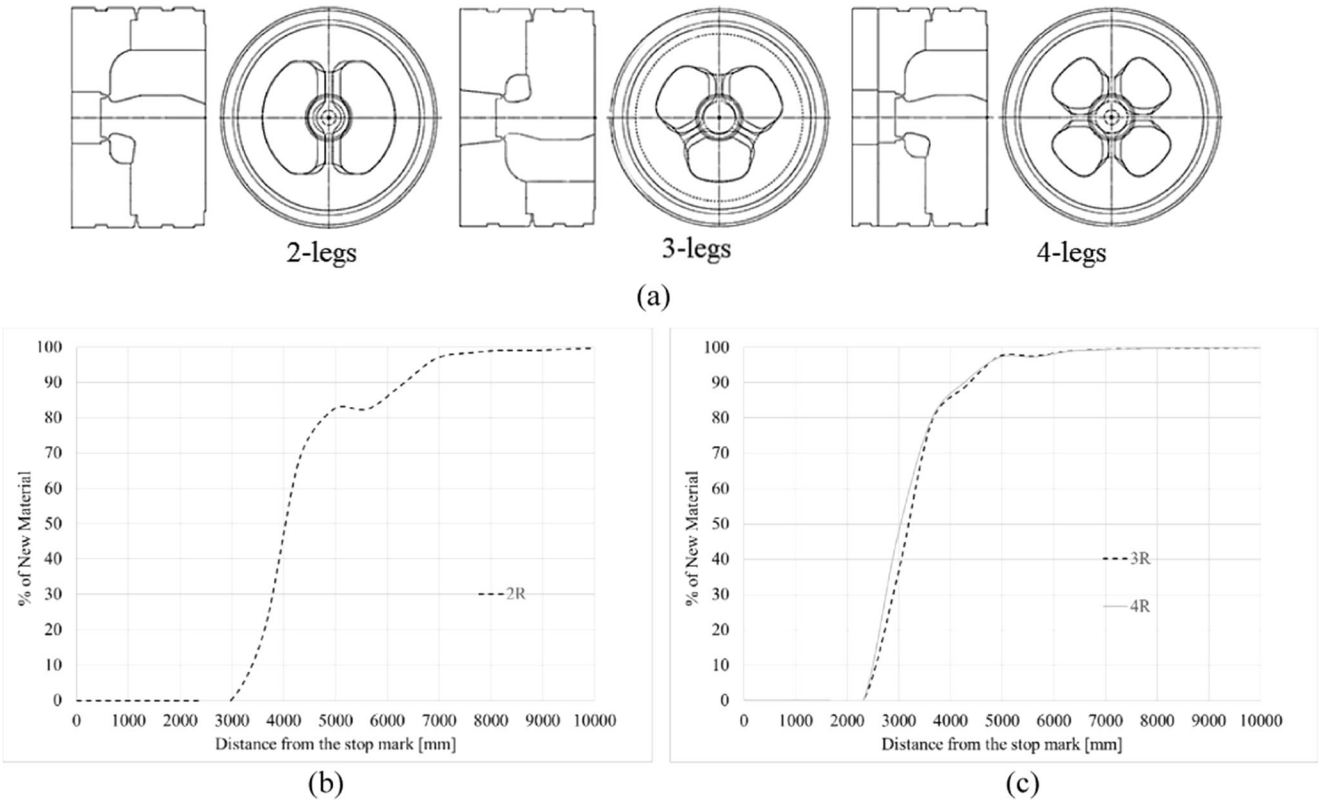

Fig. 4 **a** The three geometrical configurations of the die investigated in the second selected case study [20]; **b** the numerical evolution of the charge weld for the 2-legs, and **c** the 3–4-leg configurations as computed by means of FE models

300 mm would have mean to sell contaminated parts of the profile and/or to scrap good portions of the profiles, the former situation representing the most critical one especially in case of structural applications of the profiles.

3 Case study 2: effect of die legs

The second investigated case study consisted in a round tube profile of 51.5 mm as outer diameter and 2-mm wall thickness made of AA6005A alloy [20]. The extrusion ratio was in this case equal to 110. The effect of a different number of legs on the charge weld evolution was evaluated by means of FE transient analyses and the simulation time varied between 10.1 and 11.5 h. In this study, no experimental analyses were performed so that only analytical/numerical comparisons were made. The three geometric configurations of the die with 2, 3, and 4 legs are reported in Fig. 4a while in Fig. 4b, c, the numerically computed charge weld evolution for the 2 legs and the 3–4 legs, respectively, are shown.

Table 2 Numerical-analytical charge weld extensions (*d* in Fig. 1) for the second case study (in mm)

	Numerical (FE)		Analytical		E.R. rule
	100%	99%	(Eq. 1)	(Eq. 2)	
2 legs	13,540	8200	4827	7241	3000
3 legs	9578	6270	3400	5100	3000
4 legs	9581	6270	3349	5024	3000

As reported in detail in Table 2, for the 2-legs configuration, the FE model predicted a charge weld extension from the stop mark of 13,540 mm if the 100% of replacement is considered, reduced to 8200 mm if the 99% is accounted for. As for case study 1, Eq. 1 significantly underestimated the charge weld length. For this second case study, also Eq. 2 suggested a lower length of material to be scrapped if compared to the numerical predictions, also accounting for the 99% of replacement that was 6270 mm for both the 3 and 4-leg configurations. In addition, due to the high extrusion ratio of the round tube, the empirical rule suggested a more pronounced miscalculated scrap of material than that predicted for the first investigated case study.

4 Case study 3: effect of ports geometry

The third test case was specifically aimed at investigating the way to minimize the front-end defect by a proper die design modification but without affecting the overall process

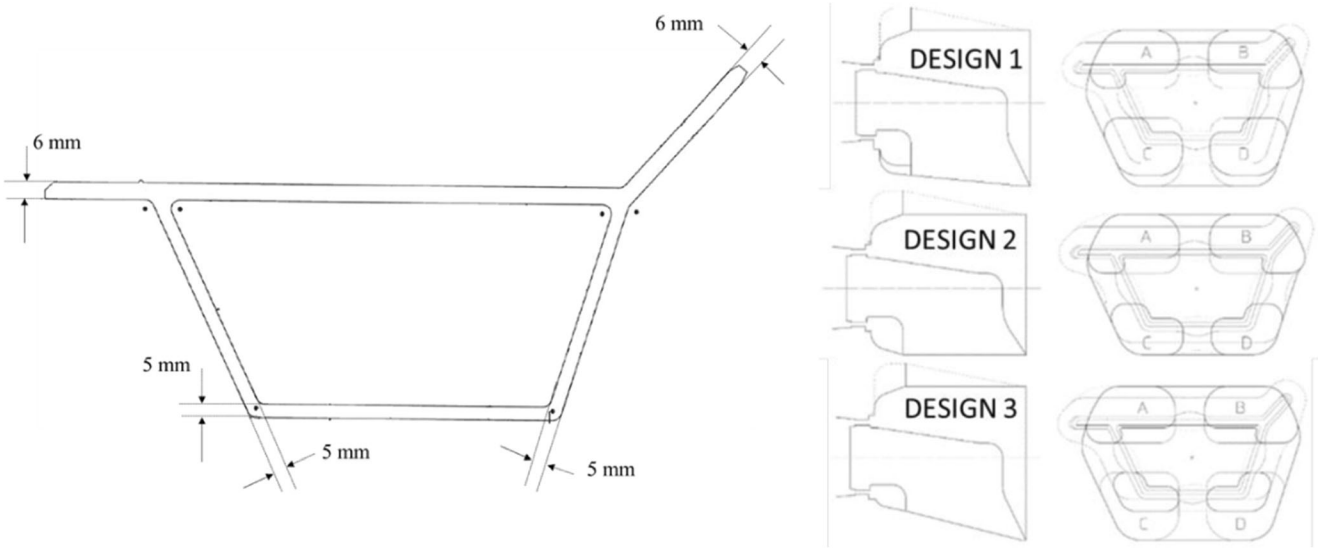

Fig. 5 The profile geometry and a sketch of the three die designs investigated in the third case study [25]

productivity for an industrial hollow profile made of AA6061 aluminum alloy (E.R. equal to 22) [25] (Fig. 5a).

Numerical and experimental data were compared for the initial die design in terms of charge weld onset and extension resulting in a very good agreement (Fig. 6). The total simulation time was 12.7 h.

Then, the impact of two modifications of the die was investigated in terms of charge weld length (Fig. 5b). In details, according to Eq. 1, design 2 was generated by imposing a "cylindrical" reduction of ports C and D to decrease the local ratio between port volumes and profile fed area while design 3 by imposing a dynamic compression of ports C and D without altering the global volume with respect to design 2. The comparison of the experimental charge weld evolution with the value suggested by rule of thumb based on the extrusion ratio once more gave evidence of its wrongness with a significant underestimation of the material to be scrapped (Table 3).

Different from what was expected on the basis of Eqs. 1 and 2 that would have suggested decreased charge weld length with decreased port volume, design 2 showed a numerical value of the increased charge weld length with respect to that of design 1 (3160 mm against 2750 mm). For design 3, even if the global volume was the same as for design 2, the FE model predicted a reduced value of the material to be scrapped while the formulas are almost the same extend. Having stated these observations, the main conclusion of the work was that material scrap is not only a matter of port volume but it is also strongly influenced by the port shape.

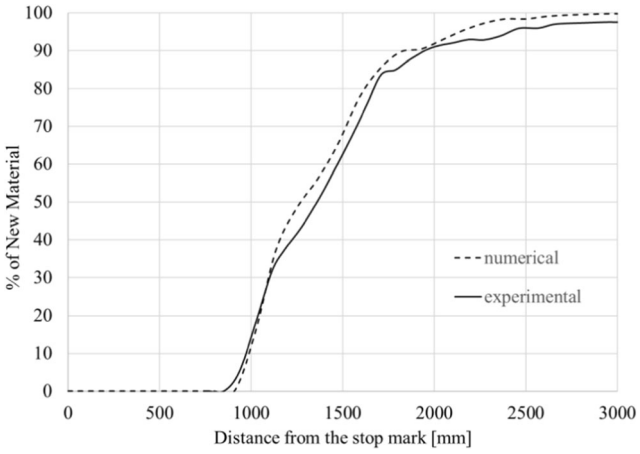

Fig. 6 Numerical-experimental comparison for the third case study [25]

5 Case study 4: effect of design strategies

The latest case study was the benchmark test of the 2017 edition of the Aluminium Two Thousand and ICEB conference [32]. The benchmark was focused on the evaluation of die design strategies for the production of two AA6005A thin C-shaped hollow profiles. The die was a porthole die and the C-shaped profiles had a variable thickness (1.8 mm and 3.6 mm) providing an extrusion ratio of 41.2 (Fig. 7). Among the many parameters monitored during the benchmark trials, the charge weld extension was furthermore experimentally evaluated.

Table 3 Numerical-experimental-analytical charge weld extensions (*d* in Fig. 1) for the third case study (in mm)

	Experimental	Numerical (FE)	Analytical		E.R. rule
			(Eq. 1)	(Eq. 2)	
Design 1	3000	2750	1573	2360	1000
Design 2		3160	1399	2098	1000
Design 3		2640	1418	2127	1000

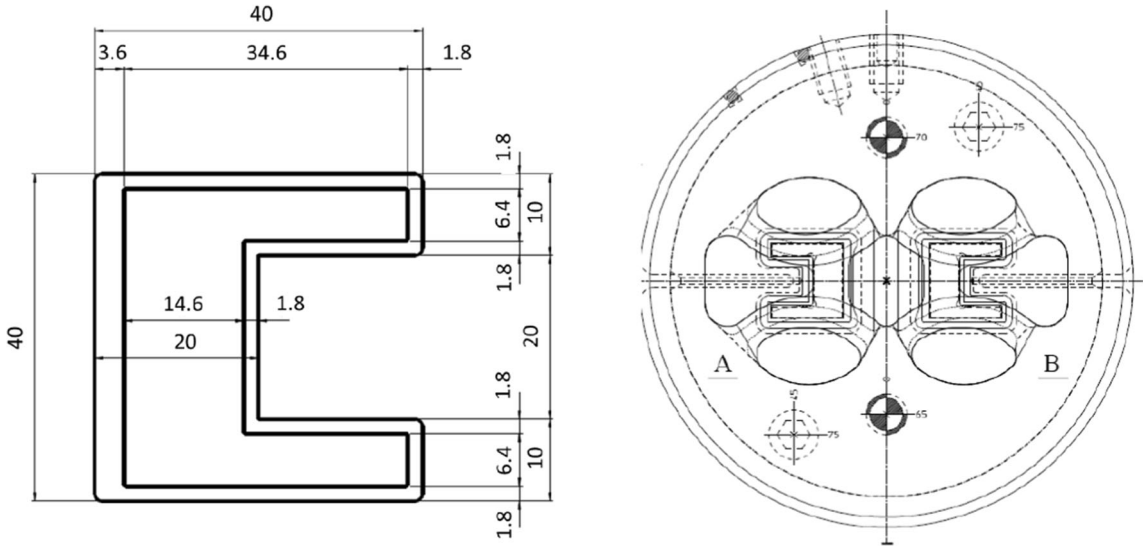

Fig. 7 The profile geometry and the porthole die design of the fourth case study [32]

The experimental-numerical comparison of the charge welds that did not differ for the two profiles A and B is reported in Fig. 8. The simulation time was in the case equal to 14.3 h. The experimental assessment of the charge welds was interrupted at 2100 mm from the stop mark corresponding to 92% of the old-new billet material replacement. At the same distance, the numerical prediction was 91% of the material replacement thus confirming a good agreement. The numerical 99% and 100% of charge weld extension was predicted at 5100 mm and 8000 mm from the stop mark respectively.

As for the previous case studies, the analytical model based on Eq. 1 considerably underestimated the experimental value of the charge weld extension (Table 4), even if not a 100% of old-new billet replacement was considered. For this latest test case, also the adjusted formula (Eq. 2) returned a poor prediction. The empirical rule based on the extrusion ratio underestimated the exhausting point as numerically computed for the 99% and the 100% of replacement. However, the direct comparison of the experimental data with the 3000 mm of material to be scrapped suggested by the empirical rule was not feasible since, as stated, the experimental acquisition ended at 2100 mm from the stop mark.

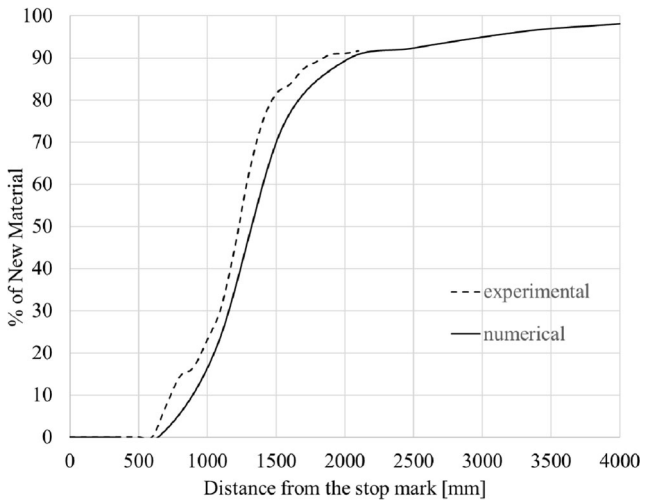

Fig. 8 Numerical-experimental comparison for the fourth case study [32]

6 Discussion

In the following, a comprehensive comparison of the four investigated case studies is reported. The percentage errors of the numerical, analytical, and empirical (E.R. rule) predictions with respect to experimental data in terms of charge weld extension (d in Eq. 1) that were available for all profiles in case study 1, for design 1 in case study 3, and for the fourth case study are shown in Table 5. For the first case study, due to the symmetry of the model, the same numerical results of profiles A and B were used in the comparison for profiles D and C respectively. The computed percentage errors of the analytical and empirical (E.R. rule) predictions with respect to numerical computed charge weld extensions due to the lack, for these specific case studies, of the experimental data are instead reported in Table 6. Since for the second case study, the numerical charge weld extensions were computed at 100% and 99% of the old-new billet replacement,

Table 4 Numerical-experimental-analytical charge weld extensions (d in Fig. 1) for the fourth case study (in mm). The reported percentage refers to the old-new billet replacement

Experimental	Numerical (FE)			Analytical		E.R. rule
	100%	99%	92%	(Eq. 1)	(Eq. 2)	
2100 (92%)	8000	5100	2000	880	1320	3000

Table 5 Percentage errors of the numerical, analytical and empirical (E.R. rule) predictions with respect to *experimental* data in terms of charge weld extension

Case study		Numerical	Eq. 1	Eq. 2	E.R. rule
1	Profile A	8.2	35.8	4.7	− 53.8
	Profile B	12.7	21.8	18.7	− 75.3
	Profile C	9.9	19.2	− 19.9	− 93.5
	Profile D	14.8	40.4	11.5	− 42.9
3	Design 1	8.3	47.6	21.3	66.7
4		4.8	25.1	− 12.4	52.4
	Avg.	9.8	31.6	4.0	− 24.4
	St. Dev	3.6	11.3	16.8	67.5

comparison are shown for both cases. As can be observed from Table 5, numerical estimations by means of FE analyses, jointly with the predictions of the adjusted Eq. 2, gave in all cases the best agreement with experimental data with average errors of 9.8% and 4.0% respectively. However, numerical models returned more robust results than Eq. 2 showing a significant lower standard deviation (3.6% with respect to 16.8%). The Eq. 1 gave in each case errors higher than 19% if compared to experimental results, with a peak error of 47.6% for the third case study. However, much higher errors were achieved by the use of the empirical rule based on the extrusion ratio with a peak under-prediction of 93.5% and a peak over-prediction of 66.7%.

Almost the same conclusions can be drawn if the comparisons are performed with respect to the numerical predictions of the charge weld extension (Table 6). In detail, Eq. 2 gave the best agreement, followed by the Eq. 1 and then by the empirical rule that returned the higher mismatched with the numerical data. The minimum percentage error was achieved for the 2-legs configuration in the second case study if the 99% of the old-new billet replacement is considered. However, this good matched significantly gets worse if the 100% of replacement is taken into account coming to 46.5% of percentage error.

Table 6 Percentage errors of the analytical and empirical (E.R. rule) predictions with respect to *numerical* data in terms of charge weld extension

Case study		Eq. 1		Eq. 2		E.R. rule	
		100%	99%	100%	99%	100%	99%
2	2 legs	64.4	41.1	46.5	11.7	77.8	63.4
	3 legs	64.5	45.8	46.8	18.7	68.7	52.2
	4 legs	66.0	46.6	49.0	19.9	69.5	52.2
3	Design 2	55.7		33.6		68.4	
	Design 3	46.3		19.4		62.1	
	Avg.	59.4	44.5	39.1	16.7	69.3	55.9
	St. Dev	8.4	2.9	12.5	4.4	5.6	6.5

In the assessment of the different predictive methods, in addition to the overall accuracy, an important role is also played by the total time required to get an estimation of the charge weld extension. This parameter becomes especially crucial if the evaluation need to be framed in an industrial context. What can be observed is that, even if the simulation time is clearly less than that of the corresponding experimental activity required for charge weld assessment, the involved transient (time-dependent) numerical analyses still implicate computational time of "some" hours for simple profiles to "some" days for more complex multi-holes products. For the four investigated case studies, the minimum required computational time was 10.1 h for case study 2, with a peak value of 132 h for case study 1. This suggests pushing the research towards novel analytical formulations of faster application that need to be developed including more die geometrical factors and process parameters for a more accurate prediction of the charge weld length.

7 Conclusions

The present work was aimed at comparing the experimental and numerical (FE) investigations performed in the years by the authors with the outcome of the analytical models nowadays reported in literature to predict the charge weld extensions. In addition, an empirical rule based on the extrusion ratio was added in the comparison in order to have a comprehensive assessment of the predictive methods nowadays available to determine the material scrap extension due to the old-new billet replacement. The final global aim of the work was the assessment of the potentialities and limits of each method and their applicability in the everyday industrial practice.

In the work, four case studies of different complexity have been considered coming to the following main findings:

- The empirical rule based on the extrusion ratio frequently adopted in the industrial practice to estimate the charge weld length returned a minimum error of 42.9% for the four investigated case studies. Thus, it was found strongly not accurate and its use is then not recommended.
- The correction of the ratio between the ports volume and the profiles cross-section area with a 1.5 factor allows for a better experimental-numerical-analytical matching in terms of charge weld extension if compared to the uncorrected formula. An average experimental-analytical percentage error of 4.0% was found for the selected case studies by using the corrected formula against 31.6% for the uncorrected one. The average numerical-analytical percentage errors were 39.1% and 59.4% with the corrected and uncorrected formulas respectively.

- In the comparisons with experimental data of the charge weld extension, the analytical formula corrected with a 1.5 factor returned an average lower percentage error (4.0%) but a higher standard deviation (16.8%) than those of the numerical predictions (average error of 9.8%, standard deviation of 3.6%).
- FE analysis represents an accurate and robust tool to predict the onset and extension of the charge welds by means of transient simulations, but the computational time can be weighty depending on the die and profile geometrical complexity. For the four investigated case studies, the minimum required computational time was 10.1 h for case study 2, with a peak value of 132 h for case study 1. This suggests pushing the research towards novel analytical formulations of faster application, especially useful in an industrial context.
- Novel analytical formulations should be developed including more die geometrical factors and process parameters for a more accurate prediction of the charge weld length

References

1. Parson NC, Hankin JD, Bryant AJ (1992) The metallurgical background to problems occurring during the extrusion of 6XXX alloys. Proc of the 5th ET Semin II 13–24
2. Bariani PF, Bruschi S, Ghiotti A (2006) Physical simulation of longitudinal welding in porthole-die extrusion. CIRP Ann 55(1): 287–290
3. Valberg H (2010) Understanding metal flow in aluminium extrusion by means of emptying diagrams. Int J Mater Form 3(1):391–394
4. Donati L, Tomesani L, Minak G (2007) Characterization of seam weld quality in AA6082 extruded profiles. J Mater Process Technol 191:127–131
5. Kim YT, Ikeda K (2000) Flow behavior of the billet surface layer in porthole die extrusion of aluminum. Metall Mater Trans A 31(6): 1635–1643
6. Valberg H (1988) Physical simulation of metal extrusion by means of model materials. Proc of the 4th ET Semin II, 321–328
7. Lefsta M, Reiso O, Johnsen V (1992) Flow of the billet surface in aluminum extrusion. Proc of the 5th ET Semin II, 503–518
8. Thackray R, Dashwood R, McShane H (2000) Simulation of the effect of tooling and billet condition on bulk and surface metal flow during extrusion. Proc of the 7th ET Semin, 213–223
9. Jowett C, Parson N, Fraser W, Hankin J, Hicklin K (2000) Simulation of flow of the billet surface into the extruded product Proc of the 7th ET Semin. I, 27–42
10. Valberg H (2002) Extrusion welding in aluminium extrusion. Int J Mater Prod Technol 17(7):497–556
11. Jowett C, Adams J, Daughetee C, Lea G, Huff OA, Fossl N (2008) Scrap allocation. Proc of the 7th ET Semin I
12. den Bakker AJ, Katgermanc L, van der Zwaag S (2016) Analysis of the structure and resulting mechanical properties of aluminium extrusions containing a charge weld interface. J Mater Process Technol 229:9–21
13. Akeret R (1992) Extrusion welds—quality aspects are now centre stage. Proc of the 5th ET Semin I:319–336
14. Finkelnburg WD, Scharf G (1992) Some investigations on the metal flow during extrusion of Al alloys. Proc of the 5th ET Semin II, 475–484
15. Loukus A, Subhash G, Imaninejad M (2004) Mechanical properties and microstructural characterization of extrusion welds in AA6082-T4. J Mater Sci 39:6561–6569
16. Nanninga N, White C, Dickson R (2011) Charge weld effects on high cycle fatigue behavior of a hollow extruded AA6082 profile. J Mater Eng Perform 20:1235–1241
17. Johannes VI, Jowett CW (1996) Transverse weld defects. Proc of the 6th ET Semin II, 89–94
18. den Bakker AJ, Werkhoven RJ, van de Nolle R (2013) Influence of die geometry on charge weld evolution, In the Proc. of the ICEB - International Conference on Extrusion and Benchmark, 57–64
19. Mahmoodkhani Y, Wells MA, Parson N, Poole W (2014) Numerical modelling of the material flow during extrusion of aluminium alloys and transverse weld formation. J Mater Process Technol 214:688–700
20. Pinter T, Reggiani B, Donati L, Tomesani L (2015) Numerical assessment of the influence of process and geometric parameters on extrusion welds and die deformation after multiple-cycles. Mater Today Proc 2(10):4856–4865
21. Yu JQ, Zhao GQ, Chen L (2016) Investigation of interface evolution, microstructure and mechanical properties of solid-state bonding seams in hot extrusion process of aluminum alloy profiles. J Mater Process Technol 230:153–166
22. Hatzenbichler T, Buchmayr B, Umgeher A (2007) A numerical sensitivity study to determine the main influence parameters on the back-end defect. J Mater Process Technol 182:73–78
23. Reggiani B, Donati L, Tomesani L (2013) Prediction of charge welds in hollow profiles extrusion by FEM simulations and experimental validation. Int J Adv Manuf Technol 69(5):1855–1872
24. Mahmoodkhani Y, Wells M, Parson N, Jowett C, Poole W (2014) Modeling the formation of transverse weld during billet-on-billet extrusion. Materials 7:3470–3480
25. Pinter T, Antonios D, Reggiani B, Gamberoni A (2016) Charge weld scrap minimization by means of dead metal flow control in die design. Proc of the 11th ET Semin. I, 827–845
26. Zhao HE, WANG H, WANG M, LI G (2012) Simulation of extrusion process of complicated aluminium profile and die trial. Trans Nonferrous Metals Soc China 22(7):1732–1737
27. Reggiani B, Donati L, Tomesani L (2017) Multi-goal optimization of industrial extrusion dies by means of meta-models. Int J Adv Manuf Manuf Technol 88:3281–3293
28. Li Q, Harris C, Jolly MR (2003) Finite element modelling simulation of transverse welding phenomenon in aluminium extrusion process. Mater Des 24(7):493–496
29. Zhang C, Dong Y, Zhao G, Chen L (2017) Experimental and numerical investigations on transverse weld of hollow aluminum profile during porthole extrusion process. Procedia Eng 207(2017): 1653–1658
30. Saha P (2008) Quality issues of hollow extrusions for aerospace applications. Proc of the 9th ET Semin.I,
31. HyperXtrude, Simulation software for extrusion process, Altair Engineering Inc. USA. http://www.altairhyperworks.com
32. Reggiani B, Donati L, Tomesani L (2017) ICEB - international conference on extrusion and benchmark. Light Metal Age 75(5): 52–60